Developmental Biology 399 (2015) 80–90

Contents lists available at ScienceDirect

Developmental Biology

journal homepage: www.elsevier.com/locate/developmentalbiology

A diffusible signal derived from hematopoietic cells supports the survival and proliferation of regenerative cells during zebrafish fin fold regeneration

Tomoya Hasegawa, Teruhiro Nakajima, Takashi Ishida, Akira Kudo, Atsushi Kawakami *

Department of Biological Information, Tokyo Institute of Technology, 4259 Nagatsuta, Midori-ku, Yokohama 226–8501, Japan

ARTICLE INFO

Article history:
Received 19 September 2014
Received in revised form
8 December 2014
Accepted 10 December 2014
Available online 19 December 2014

Keywords:
Zebrafish
Fin fold
Regeneration
Apoptosis
Myeloid
cloche
*tal*1

ABSTRACT

Multicellular organisms maintain body integrity by constantly regenerating tissues throughout their lives; however, the overall mechanism for regulating regeneration remains an open question. Studies of limb and fin regeneration in teleost fish and urodeles have shown the involvement of a number of locally activated signals at the wounded site during regeneration. Here, we demonstrate that a diffusible signal from a distance also play an essential role for regeneration. Among a number of zebrafish mutants, we found that the zebrafish *cloche* (*clo*) and *tal*1 mutants, which lack most hematopoietic tissues, displayed a unique regeneration defect accompanying apoptosis in primed regenerative tissue. Our analyses of the mutants showed that the cells in the primed regenerative tissue are susceptible to apoptosis, but their survival is normally supported by the presence of hematopoietic tissues, mainly the myeloid cells. We further showed that a diffusible factor in the wild-type body fluid mediates this signal. Thus, our study revealed a novel mechanism that the hematopoietic tissues regulate tissue regeneration through a diffusible signal.

Introduction

When tissues are injured, animals regenerate the lost or wounded parts to maintain the tissue integrity by the mechanism of tissue homeostasis, which is fundamental to multicellular organisms, but still poorly understood. In particular, many teleost fish and urodeles can regenerate limbs, tail, and fins through a process known as the epimorphic regeneration, whereas mammals are unable to regenerate lost appendages such as limbs. Unraveling the mechanism underlying the complete tissue regeneration process will help us understand the principles of tissue homeostasis and contribute to regenerative medicine.

Classical studies have shown that epimorphic regeneration involves specialized cell types, wound epidermis and the blastema. The blastema, which is induced in the underlying mesenchyme of the injured site, is a mass of proliferating cells that contribute to the principal parts of reconstituted tissues. The wound epidermis, a thick epidermis that covers the regenerating tissue, has also been thought to play an important role for regeneration (Campbell and Crews, 2008). During the past decade, studies in adult zebrafish fin regeneration have started to reveal the molecular basis of regeneration. They revealed a number of regeneration-response genes (Padhi et al., 2004; Schebesta et al., 2006) and necessary signals such as Fgf (Poss et al., 2000), Hedgehog (Quint et al., 2002), Bmp (Smith et al., 2006), Wnt (Stoick-Cooper et al., 2007), Activin (Jaźwińska et al., 2007), Igf (Chablais and Jazwinska, 2010), retinoic acid (Blum and Begemann, 2012), Notch (Grotek et al., 2013; Munch et al., 2013), and reactive oxygen species (Gauron et al., 2013).

In addition to the conventional regeneration model using adult zebrafish fin, the regeneration model using larval fin fold has been developed (Kawakami et al., 2004) and enabled us to reveal additional and complementary molecular basis (Mathew et al., 2007; Yoshinari et al., 2009; Ishida et al., 2010). Moreover, the larval fin fold model has an advantage in that genetic mutants can be tested for their regeneration phenotypes, because many zebrafish lethal mutants can survive for a relatively long period (Yoshinari et al., 2009).

Significantly, the molecules and signals so far studied in adult and larval regeneration models were the locally expressing ones that are activated in response to tissue traumas. On the other hand, it has not been known whether or not tissue regeneration could be influenced by factor(s) that are provided by other tissues away from the injured site.

In the present study, we found that the zebrafish mutant, *cloche*, which has defects in most hematopoietic and endothelial

* Correspondence to: Department of Biological Information, Tokyo Institute of Technology, B27 4259 Nagatsuta, Midori-ku,Yokohama 226-8501, Japan. Fax: +81 45 924 5718.
E-mail address: atkawaka@bio.titech.ac.jp (A. Kawakami).

http://dx.doi.org/10.1016/j.ydbio.2014.12.015
0012-1606/

cells (Stainier et al., 1995), displayed a unique regeneration defect that apoptosis occurs in the regenerative tissue. We show that the process of regeneration is initiated in the mutant; however, the primed regenerative cells do not proliferate, but undergo apoptosis. We further showed that the hematopoietic tissues, in particular the myeloid lineage cells, are essential for the survival of regenerative cells. We provided evidence that the survival of regenerative cells is normally supported by a diffusible factor that exists in the body fluid of wild-type larvae, but not that of mutant.

Materials and methods

Fish husbandry and fin amputation

Zebrafish (*Danio rerio*) were maintained in accordance with the Animal Research Guidelines at Tokyo Institute of Technology. Zebrafish were maintained in a re-circulating system with a 14 h (hrs)/day and 10 h/night cycle at 28.5 °C. Fin fold amputation was performed as previously described (Kawakami et al., 2004). For wound healing assay, the larval fin fold was punctured with a fine glass capillary (tip diameter, 20 μm). After amputation, larvae were incubated in egg water (0.06% artificial marine salt, 0.0002% methylene blue) and subjected to the respective analyses. The zebrafish strains used in this study are wild-type strain, TL, and mutant strains, *tal1*^{t21384}, *tp53*^{zdf1}, *vlad tepes*^{vltm651}, *clo*^{m39}, and *clo*^{la1164}.

Fish genotyping

Genotype of *tal*1 mutant was determined according to the previously described protocol (Bussmann et al., 2007). Genotyping of *tp53*^{zdf1} was performed according to the protocol supplied by the Zebrafish International Resource Center (ZIRC) using primers (TPA03: 5'-ACATGAAAT TGCCAGAGTATGTGTC-3'; TPA04: 5'-TCGGATAGCC-TAGTGCGAGC-3'). The PCR products were digested with MboII and analyzed the restriction length polymorphism. Genotype of *cl* ^{m39} was determined by the PCR using the linked markers, *z*1496 and/or *z*8617.

Whole-mount in situ hybridization (ISH) analysis

Whole-mount ISH analysis was performed according to the protocol by Thisse and Thisse (2008). After detection of ISH signal, the samples were fixed with 4% paraformaldehyde (PFA) in phosphate-buffered saline (PBS) for color preservation, equilibrated with 80% glycerol, and mounted on slide glasses for inspection and taking photographs. The ISH probes used in this study were previously described (Yoshinari et al., 2009)

Whole-mount immunohistochemistry

Zebrafish larvae were fixed with 4% PFA in PBS at 4 °C for overnight, washed three times with PBS supplemented with 0.1% Triton X-100 (PBTx), dehydrated with methanol, and stored at −30 °C. Samples were rehydrated with PBTx and blocked with the blocking buffer (5% serum and 0.2% bovine serum albumin in PBTx) for 2 h at room temperature (RT). Subsequently, the samples were reacted with anti-DsRed antibody (1:1000 dilution; Clontech) at 4 °C for overnight. Following extensive washing with PBTx (10 min × 6 times) at RT, the samples were incubated with Alexa555-conjugated secondary antibodies at 4 °C for overnight. After washing with PBTx, the tail regions were isolated and mounted in 80% glycerol containing 2.5% 1,4-diazabicyclo [2,2,2] octan (Nacalai Tesque) as an anti-fading reagent. Fluorescent pictures were acquired by a confocal microscopy.

Chemical inhibitors

The DNA polymerase inhibitor, Aphidicolin (Wako), was used at 100 μM. The VEGF receptor inhibitor, PTK787 (vatalanib; JS Research Chemical Trading; Chan et al., 2002), was used at 5 μM. The ROS inhibitors, VAS2870 (Sigma; Niethammer et al., 2009) and apocynin (Merck; Love et al., 2013), were used at 5 and 100 μM, respectively. The JNK inhibitor, SP600125 (Tocris; Ishida et al., 2010), was used at 10 μM. The inhibitors were dissolved in dimethylsulfoxide as stock solutions (at least 1000 × concentrations of respective working concentrations) and stored at −30 °C. Inhibitors were diluted with egg water before use. PTK787 was applied at 10 h post fertilization. Other inhibitors were applied to zebrafish larvae at least 1 h before fin fold amputation.

Cell proliferation analysis

Proliferating cells were labeled with 5-Bromo-2-deoxyuridine (BrdU; 5 mM). The larvae were fixed with 4% PFA for 2 h at RT, dehydrated with methanol and stored at −30 °C. Immunochemical detection was performed as described previously (Yoshinari et al., 2009). The BrdU-labeled cells were quantified from the acquired confocal images.

Terminal deoxynucleotidyl transferase dUTP nick end labeling (TUNEL) staining

Larvae were fixed with 4% PFA at 4 °C for overnight, dehydrated with methanol, and stored at −30 °C. Detection was performed using an *in situ* apoptosis detection kit (Roche). Briefly, the samples were rehydrated with PBTx, treated with 10 μg/ml Proteinase K in PBTx for 3 min at RT, washed with PBTx, and refixed with 4% PFA in PBS for 20 min. The samples were further incubated in a freshly prepared 0.1% sodium citrate, 0.1% Triton X-100 on ice for 15 min, washed with PBTx, and reacted with the TUNEL reaction mixture at 37 °C for 1 h. The reaction was terminated by washing with PBTx. The samples were mounted under 80% glycerol and observed under a fluorescence microscope.

Sudan Black B staining for neutrophils

Larvae were fixed with 4% formaldehyde in PBS for 1 h at RT, rinsed with PBS, and incubated in 0.03% Sudan Black B (Sigma). After extensive washing with 70% ethanol and rehydration with PBS+0.1% Tween 20, samples were mounted with 80% glycerol.

Injection experiments

Injections were performed according to a standard procedure. Fertilized zebrafish eggs were dechorinated with 2% pronase (Roche) and used for microinjection during the 1- to 4-cell stages. Antisense morpholino oligonucleotides (MO) used in this study are:

tnnt2a-MO (5′-CATGTTTGCTCTGATCTGACACGCA-3′);
*pu.*1-MO (5′-GATATACTGATACTCCATTGGTGGT-3′);
*tal*1-MO (5′-AATGCTCTTACCATCGTTGATTTCA-3′);
standard control (std) MO (5′-CCTCTTACCTCAGTTACAATTTATA-3′).

For mRNA injection, the mRNA was synthesized *in vitro* from the linearized plasmid, pCS2-*EGFP-bcl*2 (Langenau et al., 2005), using the mMessage Machine kit (Ambion), and injected at 1–4 cell stages (0.5 nl of 0.5 μg/μl solution) into fertilized eggs obtained by incrosses of *clo* heterozygous fish.

Cell transplantation

Wild-type or *clo* heterozygous fish carrying the transgene *Olactb:* loxP-DsRed-loxP-EGFP (Yoshinari et al., 2012) was mated

to obtain embryos. Embryos with DsRed fluorescence were used as donors and transplanted cells into wild-type or *clo* embryos. Cell transplantation was performed at the dome stage according to a standard procedure. Operated embryos were cultured in 0.3 × Danieau buffer (17 mM NaCl, 2 mM KCl, 0.12 mM $MgSO_4$, 41.8 mM $Ca(NO_3)_2$, 21.5 mM HEPES, pH 7.6) supplemented with 10,000 units/ml penicillin G and 10 mg/ml streptomycin sulfate at 28.5 °C until 2 dpa. At this stage, the genotype of donor and host embryos was judged according to the *clo* heart phenotype. Embryos with many transplanted cells in fin fold were subjected to fin fold amputation and TUNEL analysis.

Tail explant culture and acridine orange staining of apoptotic cells

The tail tissue was isolated from 2 dpf larvae by cutting the trunk at a site posterior to the yolk extension with a scalpel in the L15 medium. The explants were extensively washed with L15 medium, placed in the L15 medium containing 10% fetal calf serum, penicillin G and streptomycin, and incubated at 28.5 °C. Seven explants were cultured in 100 µl of medium using the 96-well plate. To detect apoptosis, the cultured explants at 12 hpa were placed in 5 µg/ml acridine orange (Sigma) in L15 medium at RT for 30 min, and washed with L15 medium (3 times × 5 min). Samples were mounted on glass slides and immediately subjected to image acquisition.

Preparation of body extract

For preparing the body extract, zebrafish larvae (2–3 dpf) were collected and gently squashed in the L15 culture medium with a homogenizer. After centrifugation at 4 °C for 10 min, the supernatant, adjusted to a concentration of one larva equivalent per microliter, was sterilized through a syringe filter unit (Millex HV13, 0.45 µm, Millipore), and stored at −20 °C. The cell survival activity was assayed by adding the diluted extract (1 larvae/µl) to the *clo* or *tal*1 mutant explant culture in 96-well plate. For heat treatment, the extract was incubated at 80 °C for 20 min and centrifuged for 10 min at 4 °C.

Results

A unique regeneration phenotype of the cloche mutant

Using the fin fold regeneration model, we found that *cloche* (*clo*), a zebrafish mutant originally identified from a phenotype that lacks most hematopoietic and endothelial cells (Stainier et al., 1995), displayed a regeneration defect (Fig. 1A). Fin fold tissue is normally restored to the original shape and size by three days post amputation (dpa) (Kawakami et al., 2004); however, the *clo* mutant displayed an apparent regeneration defect accompanying a unique blister-like tissue appearance (arrowheads in Fig. 1A). We speculated that this might represent dying cells and their debris, and indeed many TUNEL-positive cells were detected in the region where regeneration will normally take place (Fig. 1B). In contrast to the amputated *clo* fin fold, only a few TUNEL-positive cells were observed in the uncut mutant fin fold up to five days post fertilization (Supplementary Fig. S1A and B), indicating that the cell death in the mutant is regeneration-dependent.

To further confirm that the cell death in the *clo* mutant is regeneration-dependent, we performed a wound healing assay, in which a small hole was made in fin fold (Supplementary Fig. S1C). Both in wild-type and *clo* mutant, a hole in the fin fold was rapidly restored and became almost invisible before 12 hpa. The BrdU labeling in wild-type showed that no significant cell proliferation occurred in the punctured fin fold (Supplementary Fig. S1D), indicating that the assay induced wound healing without regenerative cell proliferation as is the case of slit assay in adult fin (Gauron et al., 2013). In this assay, no significant increase of TUNEL-positive cells was observed in the *clo* mutant (Supplementary Fig. S1D), confirming that the observed apoptosis in the mutant depend on the wound type that followed by regenerative cell proliferation.

Further, the BrdU labeling of amputated fin fold showed that regenerative cell proliferation was also severely reduced in the mutant. Only a few BrdU-labeled cells were detected in the mutant even after long BrdU labeling up to 24 h post amputation (hpa) (Fig. 1C). This suggests that cells in the mutant fin fold did not initiate regenerative cell proliferation in the first place. Despite the defect in the regenerative tissue, a normal level of BrdU labeling was observed in the head and trunk regions of the mutant (Supplementary Fig. S2), indicating that the *clo* mutation affected cell proliferation only in the regenerative tissue. In contrast to amputated fin fold, cell proliferation in the uncut fin fold was very few and indistinguishable between wild-type and mutant (Supplementary Fig. S1G and H). Together, these data indicate that both of apoptosis phenotype and cell proliferation defect in the *clo* mutant are regeneration-dependent.

Since the above analyses used the clo^{tm39} allele which contains a large deletion in the chromosome 13 (Liao et al., 2000), we wanted to know whether or not the *clo* gene itself is responsible for the phenotype. To confirm it, we used another *clo* allele, *la*1164, which was generated by *N*-ethyl-*N*-nitrosourea mutagenesis and thought to be a point mutation (Sakaguchi et al., 2008). The clo^{la1164} allele showed indistinguishable regeneration phenotypes in both cell death and defect of cell proliferation (Supplementary Fig. S3), indicating that the *clo* gene itself is responsible for these phenotypes.

Cell death in the clo mutant is the apoptosis

Cell death occurs by a number of different mechanisms, such as necrosis, apoptosis, and autophagy (Kroemer et al., 2008; Miura, 2011). Normally, tissue amputation will immediately induce necrotic cell death by unrecoverable damage to cells. Actually, with TUNEL analysis, we observed many cell deaths at 0.5 hpa in the injured region of both wild-type and *clo* mutant (Fig. 2A and B). Though this necrotic cell death disappeared by 6 hpa, many TUNEL-positive cells were again detected from 12 hpa only in the *clo* mutant (Fig. 2A and B). This delayed occurrence of cell death suggested that the *clo*-specific cell death is not a necrotic one.

To reveal whether or not the cell death is regulated by an apoptosis program, we overexpressed the Bcl2, a negative regulator in many apoptosis pathways (Mohamad et al., 2005), in the *clo* mutant. When homozygous mutants were injected with the mRNA encoding the *EGFP-zbcl2* (Langenau et al., 2005), TUNEL-positive cells were significantly decreased (Fig. 3A and B), indicating that cell death in the *clo* mutant is caused by a Bcl2-regulated apoptosis pathway.

We further examined the involvement of tp53, a central regulator for executing apoptosis (Vousden, 2000), in the *clo* apoptosis. It has been shown that the *tp*53 mutation reduced the irradiation-induced apoptosis (Berghmans et al., 2005); however, the apoptosis in the amputated fin fold of *clo* and *tp*53 double mutants was indistinguishable from that of *clo* mutant (Fig. 3C and D), indicating that the apoptosis in the mutant is executed by a tp53-independent atypical pathway.

Moreover, we investigated the role of reactive oxygen species (ROS) such as hydrogen peroxide (H_2O_2) and Jun N-terminal kinase (JNK), because the ROS signaling could trigger pathways responsible for apoptosis and JNK activation (Gauron et al., 2013). However, the JNK inhibitor, which specifically impacts on the JNK signaling and results in the suppression of fin fold regeneration under the used condition (Ishida et al., 2010; Supplementary

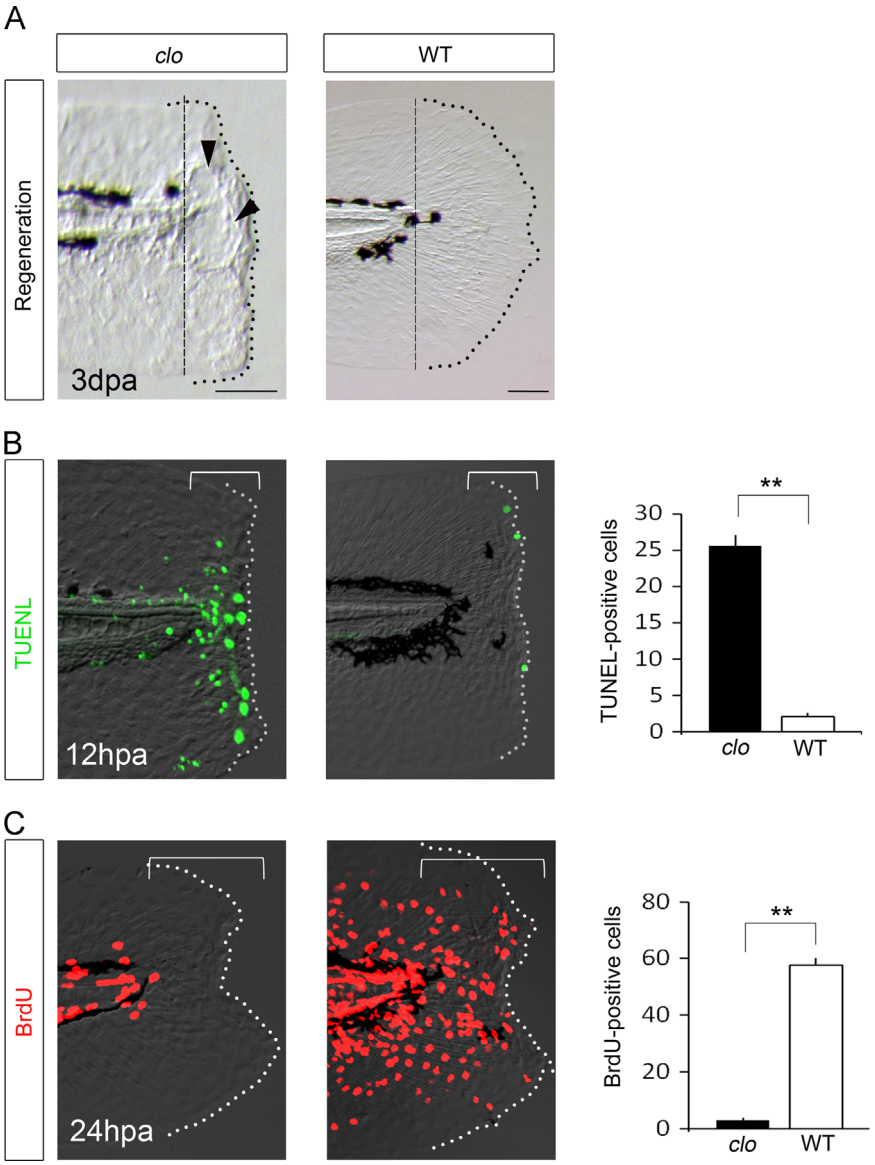

Fig. 1. Unique regeneration defects in the *clo* mutant. (A) Impaired fin fold regeneration in the *clo* mutant and normal regeneration in the sibling wild-type. The arrowheads mark the characteristic blister-like structures often observed in the amputated mutant tissue. The dashed line indicates the site of amputation. (B) TUNEL analysis of amputated fin fold of *clo* mutant and sibling wild-type at 12 hpa. The graph in the right shows the quantification of TUNEL-positive cells in the *clo* mutant ($n=25$) and wild-type ($n=28$) in the regeneration-responsive region (brackets). (C) BrdU analysis of cell proliferation. The BrdU labeling was performed 0–24 hpa. The graph shows the quantification of BrdU-positive cells in *clo* mutant ($n=7$) and wild-type ($n=7$) in the bracketed regions. Data are presented as mean ± s.e.m. Statistical significance was tested using Welch's *t* test. $^{**}P<0.001$. The dotted lines indicate the outline of the fin fold. Scale bars for *clo* and wild-type represent 50 μm, respectively. dpa, days post amputation; hpa, hours post amputation.

Fig. S4A), did not affect the *clo* apoptosis (Supplementary Fig. S4B and C). Likewise, the ROS inhibitors, which are also able to suppress the ROS signaling and impair regeneration (Love et al., 2013; Yoo et al., 2012; Supplementary Fig. S4A), neither affected the *clo* apoptosis (Supplementary Fig. S4B and C). Thus, it is suggested that the apoptosis in the *clo* mutant is not mediated by the ROS and JNK signalings.

Intriguingly, the *clo*-specific apoptosis coincides with the stage when regenerative cell proliferation begins (Ishida et al., 2010; Kawakami et al., 2004). Therefore, we thought that regeneration program was somehow initiated or primed in the mutant. To confirm this, we conducted ISH analysis of *junb* and *junbl*, early markers induced in the wound epithelium and the blastema, respectively (Yoshinari et al., 2009), and observed that these genes were actually induced in the *clo* mutant (Fig. 3E). Although the expression of regeneration-induced genes were slightly higher, tissue appearance and wound closure process looked normal. In addition, histological analysis showed that the apoptosis predominantly localized in the mesenchymal region (Fig. 3F), where the regenerative cell proliferation mainly occurs. Taken together, these data suggest that the cell death in the *clo* mutant is the apoptosis of primed regenerative cells caused by an atypical signaling pathway that does not depend on Tp53, ROS, or JNK.

Non-cell autonomous action of clo gene function for blastema survival

We next asked if the Clo protein directly required for the survival of regenerative cells. To investigate the cell autonomy of Clo function during regeneration, we performed cell transplantation experiments between *clo* and wild-type embryos and detected apoptosis after fin

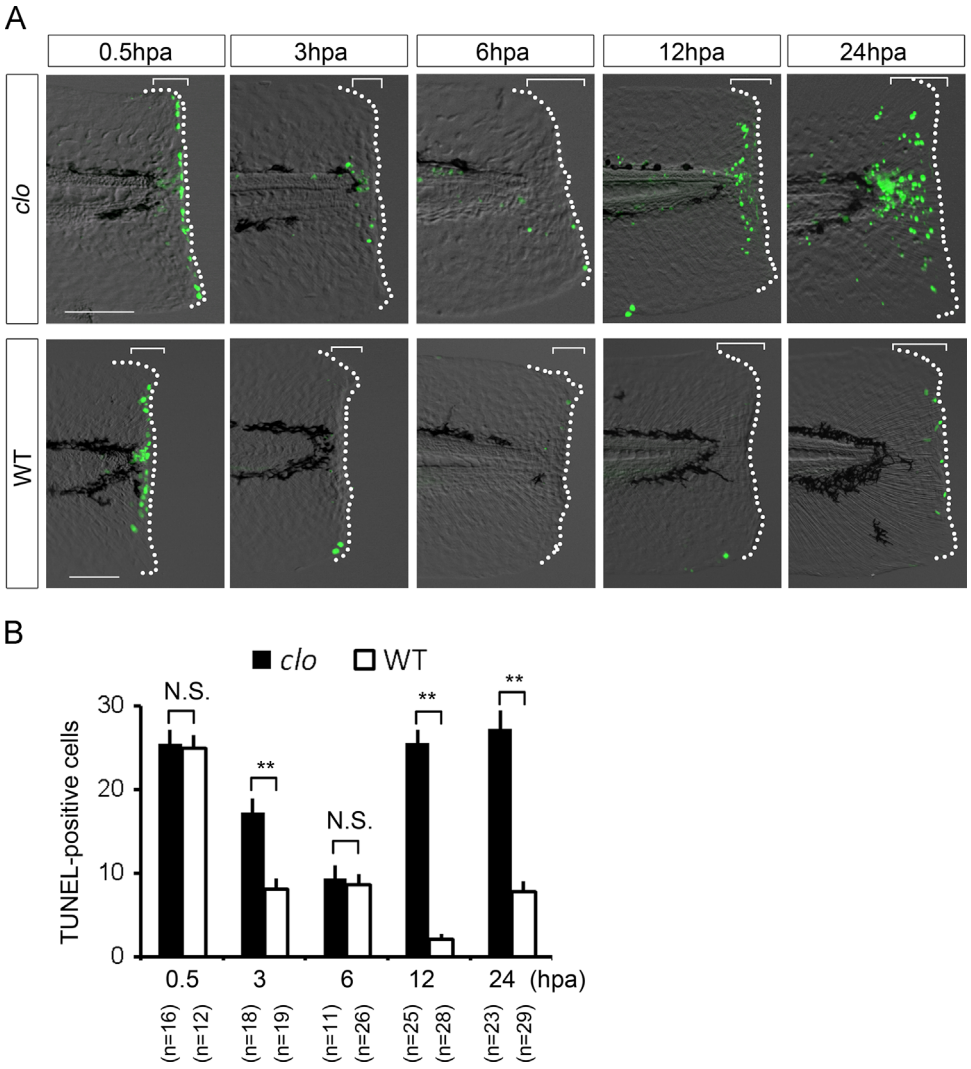

Fig. 2. Temporal change of cell death in the *clo* mutant and wild-type after fin fold amputation. (A) TUNEL analysis of cell death at respective stages of fin fold regeneration in the *clo* mutant and wild-type. Note that mutant-specific cell death was only observed at 12 hpa and afterward. Scale bars for *clo* and wild-type represent 100 μm, respectively. (B) Quantification of TUNEL analysis. The TUNEL-positive cells in the bracketed areas in (A) were scored. Data are presented as mean ± s.e.m. Statistical significance was tested using Welch's *t* test. $^{**}P < 0.001$.

fold amputation (Supplementary Fig. S5A). When *clo* mutant cells were transplanted into wild-type embryos, almost no apoptotic cells were detected in spite of the presence of many mutant cells in the fin fold (Supplementary Fig. S5B). Conversely, when wild-type cells were transplanted into *clo* larvae, apoptosis was induced in many wild-type donor cells as well as in the mutant host cells (Supplementary Fig. S5C). These results suggested that the Clo function is non-cell autonomous for the survival of regenerative cells.

However, the transplantation experiment was so tough to obtain enough numbers of successful transplantations that carry lots of transplanted cells within fin fold. However, the above suggestion of non-cell autonomous action of Clo prompted us to speculate that the lack of hematopoietic cells in the mutant is responsible for cell survival. To test this idea, we looked at the phenotype of another hematopoietic mutant, *tal*1. The *tal*1 gene has been suggested to function downstream of *clo* and regulate hematopoietic cell differentiation (Liao et al., 2000). Importantly, the *tal*1 mutant and morphant also displayed apoptosis of regenerative cells and defect of cell proliferation during fin fold regeneration (Fig. 4; Supplementary Fig. S6). This result strongly supported the notion that the hematopoietic and/or endothelial cells are essential for the survival of regenerative cells.

Myeloid cells are required for blastema survival

Hematopoietic lineage cells contain several distinct cell types (Jing and Zon, 2011). We sought to further specify the cell types required for the survival of regenerative cells. We first used the *vlad tepes* mutant (Lyons et al., 2002), a mutant of *gata*1 transcription factor, to test the role of red blood cells, but the apoptosis in the amputated fin fold was not detected in the *vlad tepes* mutant (Fig. 5A and D).

We next knocked down the endothelial cells by using PTK787, an inhibitor against the vascular endothelial growth factor receptor (VEGFR) (Chan et al., 2002), but in spite of the reduction of endothelial cells and network of blood vessels (Supplementary Fig. S7A), we did not detect the apoptosis of regenerative cells (Fig. 5B and D).

Furthermore, we knocked down the myeloid lineage cells by using the MO against *pu*.1, a gene encoding the transcription factor for myeloid cell differentiation (Rhodes et al., 2005). Importantly, the *pu*.1 knockdown larvae clearly displayed both the apoptosis of regenerative cells and impaired cell proliferation as in the *clo* or *tal*1 mutants (Fig. 5C–F; Supplementary Fig. S7B), indicating that myeloid cells have a major role for the survival of regenerative cells.

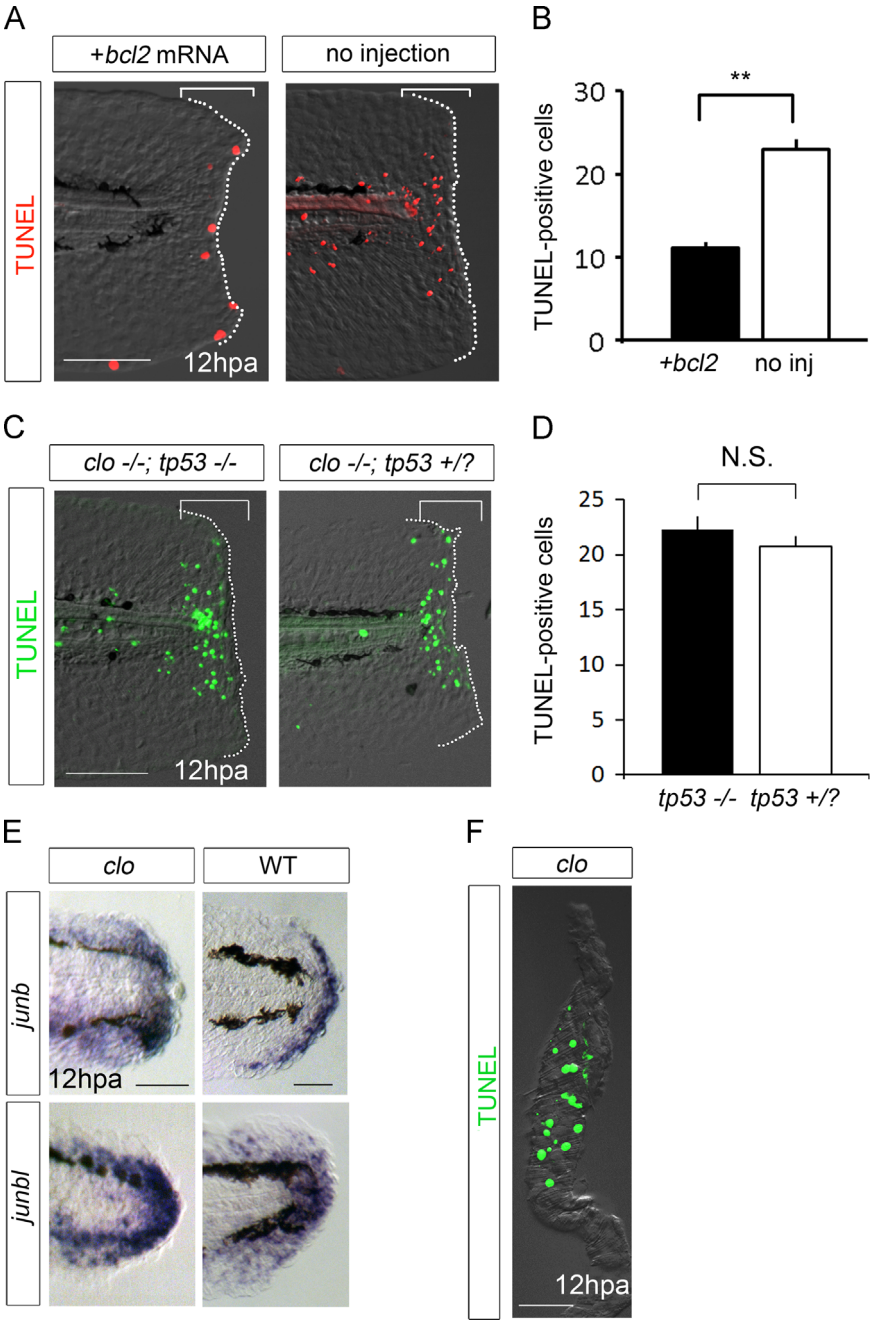

Fig. 3. Cell death in the *clo* mutant is the apoptosis of primed regenerative cells. (A) TUNEL analysis during fin fold regeneration in the *clo* larvae that was injected or uninjected with *bcl2* mRNA. *clo*-specific cell death (brackets) was significantly suppressed by Bcl2 overexpression. (B) Quantification of TUNEL-positive cells in (A). $n=12$ (injected) and 8 (uninjected), respectively. Data are presented as mean ± s.e.m. Statistical significance was tested using Welch's *t* test. $^{**}P<0.001$. (C) TUNEL analysis in the double mutants of *clo* and *tp*53. Apoptosis in the *clo* mutant (brackets) was not affected by the absence of tp53. (D) Quantification of the number of TUNEL-positive cells in (C). $n=14$ ($clo^{-/-}$; $tp\ 53^{-/-}$) and 27 ($clo^{-/-}$; $tp53^{+/?}$), respectively. (E) ISH analysis of *junb* and *junbl*, markers of the wound epidermis and blastema, respectively. Both markers were expressed in the *clo* mutant at higher levels than wild-type ($n=7/7$, respectively). (F) Horizontal cross section of *clo* fin fold that were made after TUNEL staining. Predominant localization of TUNEL-positive cells in the mesenchymal region in the *clo* mutant. The dotted lines in (A) and (C) indicate the outlines of fin folds. Scale bars represent 100 μm in (A) and (C), and 50 μm in (E) and (F).

Blastema survival is supported by a diffusible factor in the body

Given the essential role of hematopoietic cells for the survival of regenerative cells, we further investigated how the signal is mediated from the hematopoietic tissues to wounded site. To do this, we developed an *in vitro* assay using the tail explant, in which the tail tissue caudal to the yolk extension was isolated and placed in the culture media until 12 hpa (Fig. 6A). The cultured tail tissues of wild-type larva neither showed morphological abnormalities nor increased apoptosis (Supplementary Fig. S8). They also expressed the regeneration-associated genes, *junbl* and *junb* (Supplementary Fig. S9), indicating that the tail explants retained the primed regeneration status *in vitro* up to 12 hpa. Importantly, the absence of apoptosis in the wild-type explants suggests that apoptosis is not caused by impaired circulation in the *clo*/*tal*1 mutants. We further confirmed this by knocking down the *tnnt2a*/*silent heart*, a gene necessary for heart beat (Sehnert et al., 2002), but apoptosis was not observed in the morphant (Fig. 6C and D).

We next cultured the explants from *clo* or *tal*1 mutants and observed that the apoptosis phenotype was perfectly reproduced

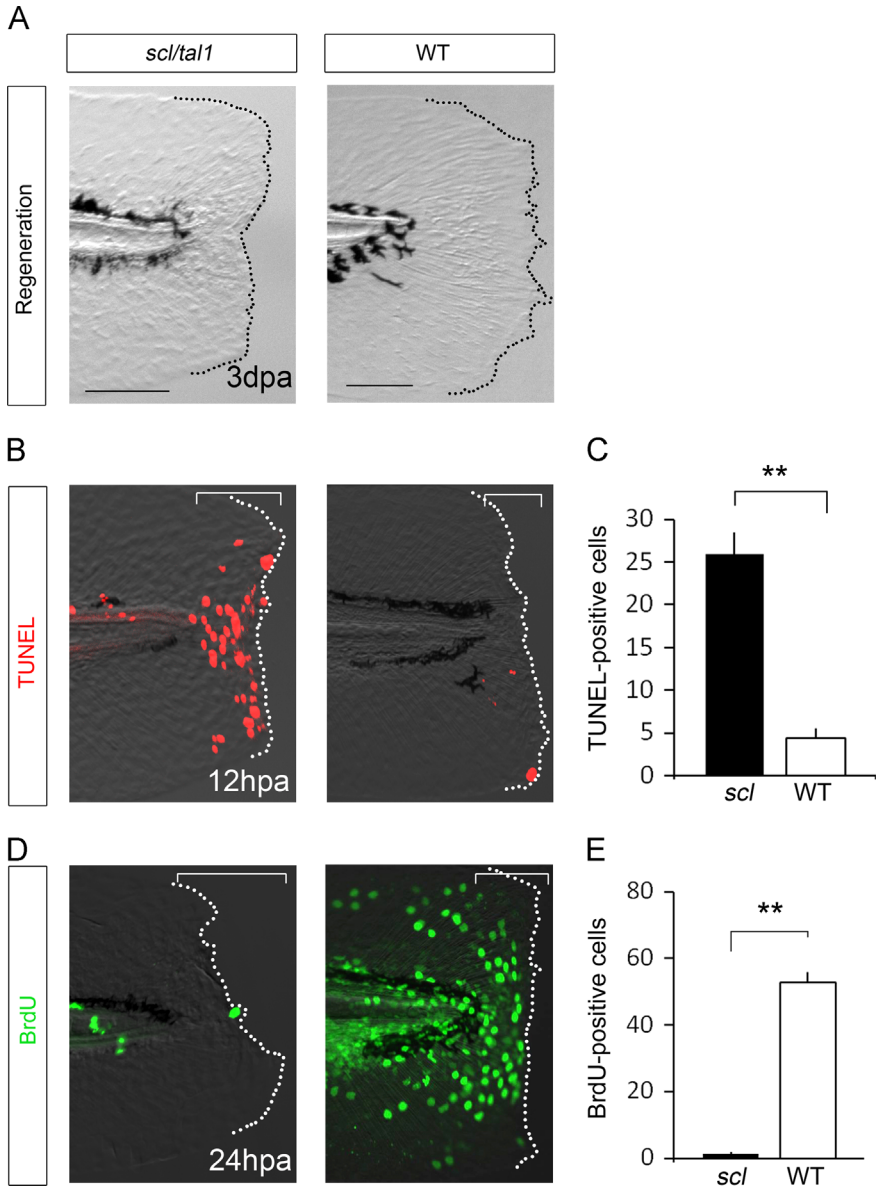

Fig. 4. Regeneration phenotype in the *tal*1 mutant. (A) Regeneration of fin fold in the *tal*1 mutant and sibling wild-type at 3 dpa. Regeneration in the *tal*1 mutant was severely impaired. (B) TUNEL analysis of amputated fin fold in the *tal*1 and sibling wild-type at 12 hpa. (C) Quantification of TUNEL analysis. The graph shows the number of TUNEL-positive cells in the *tal*1 mutant ($n=18$) and wild-type ($n=10$). (D) BrdU analysis of cell proliferation of amputated fin fold in the *tal*1 and sibling wild-type. The BrdU labeling was performed 0–24 hpa. (E) Quantification of BrdU-positive cells. The graph shows the number of BrdU-positive cells in the *clo* mutant ($n=6$) and wild-type ($n=7$). The number of TUNEL and BrdU-positive cells was quantified in the bracketed areas. Data in (C) and (E) are presented as mean ± s.e.m. Statistical significance was tested using Welch's *t* test. $^{**}P<0.001$. The dotted lines indicate the outline of the fin fold. Scale bars for *clo* and wild-type represent 100 μm, respectively.

in vitro (Fig. 6B) and indistinguishable between two mutants (data not shown). Using the explants from the mutant, we assessed if the body extract prepared from wild-type or *tal*1 mutant could rescue the apoptosis in the mutants. The body extract prepared from the wild-type larvae rescued the apoptosis of regenerative cells in the *tal* mutant, but the body extract from the *tal*1 mutant did not (Fig. 6E and F). The result indicates that the survival of regenerative cells is supported by a diffusible factor in the wild-type body.

To further assess the nature of survival factor, we incubated the extract at 80 °C for 20 min and tested for the anti-apoptosis activity. The heat-treated extract still rescued the apoptosis of the mutant tail explants, and no significant decrease of the activity was observed (Supplementary Fig. S10A). Moreover, we also asked if the amount of factor is increased upon tissue wound. We prepared extracts from amputated and uncut larvae, respectively, and compared the amount of anti-apoptosis activity using serially diluted extracts. However, no significant difference was observed between extracts from amputated and uncut larvae (Supplementary Fig. S10B). Taken together, the data suggest that the survival factor is a heat-stable substance that exists in the body fluid irrespective of regeneration status.

Discussion

We have previously established the fin fold regeneration assay as an experimental system to investigate the regeneration mechanism (Kawakami et al., 2004). This system enabled us to utilize the zebrafish mutants and analyze their effects on regeneration (Yoshinari et al., 2009). Here, we found that the zebrafish mutants, *clo* and *tal*1, which lack most of hematopoietic and endothelial cells, showed apoptosis of regenerative cells. Our study revealed that a

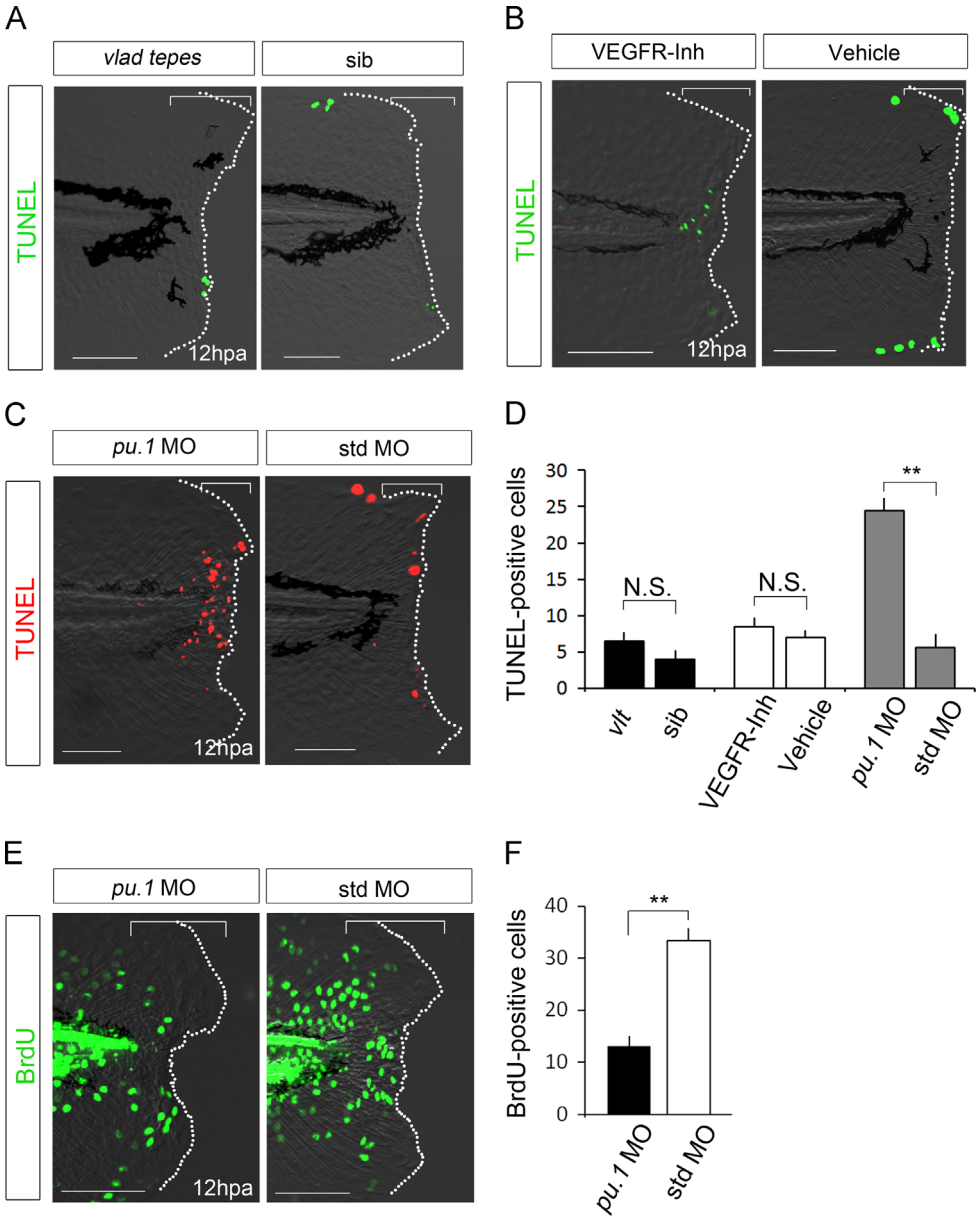

Fig. 5. Role of myeloid cells for the survival of regenerative cells. (A) TUNEL analysis of amputated fin fold in the *vlad tepes* mutant that lacks the red blood cells ($n=21$) and sibling wild-type ($n=8$) at 12 hpa. No significant increase of apoptotic cells was observed. (B) TUNEL analysis of amputated fin fold in the wild-type larvae treated with VEGFR inhibitor, PTK787 ($n=39$) or control vehicle ($n=9$). Impairment of blood vessel formation by the inhibitor did not induce apoptosis. (C) TUNEL analyses of amputated fin fold in larvae injected with the *pu.*1 MO ($n=23$) and control standard MO ($n=7$). Note the increase of TUNEL-positive cells in the *pu.*1 MO-injected larvae. (D) Quantification of TUNEL analyses (brackets) in (A–C). Data are presented as mean ± s.e.m. Statistical significance was tested using Welch's *t* test. $^{**}P<0.001$. N.S., not significant. (E) BrdU analyses of amputated fin fold in larvae injected with the *pu.*1 MO ($n=9$) and control standard MO ($n=10$). (F) Quantification of BrdU analyses (brackets) in (E). Data are presented as mean ± s.e.m. Statistical significance was tested using Welch's *t* test. $^{**}P<0.001$. The dotted line indicates the outline of the fin fold. Scale bars represent 100 μm.

diffusible factor derived from the hematopoietic cells supports the survival and proliferation of primed regenerative cells (Fig. 7).

Intriguingly, the apoptosis phenotype in the *clo* and *tal*1 mutants always accompanies a defect of cell proliferation (Figs. 1C and 4D). It may mean that apoptosis and survival/proliferation are alternative cell fate, though the exact identity between the apoptotic cells in mutants and proliferating cells in wild-type larvae is still uncertain. In either cases, it is thought that cells in the regenerative tissue are susceptible to apoptosis once they are activated by the regeneration-inducing signal. An important difference of regenerative cells from non-regenerative cells could be a fast cell cycle. As we previously observed, cells in the zebrafish fin fold at 2 dpf already cycle slowly, but re-enter the fast cell cycle in response to amputation (Kawakami et al., 2004). Fast cell cycle in regenerative cells might make them sensitive to apoptosis through a mechanism that fast cycling cells such as tumor cells are removed by apoptosis (Vousden and Lane, 2007). Therefore, the survival factor that we found in the present study could counteract the endogenous apoptosis-inducing signal and authorize the regenerative cells to enter the cell proliferation cycle. On the other hand, it appears that survival of regenerative cells is not sufficient for executing cell proliferation. Because, cell proliferation can be suppressed without inducing apoptosis by an inhibitor of DNA synthesis (Supplementary Fig. S11). In addition, as we have previously showed, the zebrafish mutants of *hspa*9 and *smarca*4 genes displayed reduced cell proliferation in spite of the survival of regenerative cells (Yoshinari et al., 2009). Thus, the signal from the hematopoietic tissues can support cell survival, but additional signals may be required for subsequent cell proliferation.

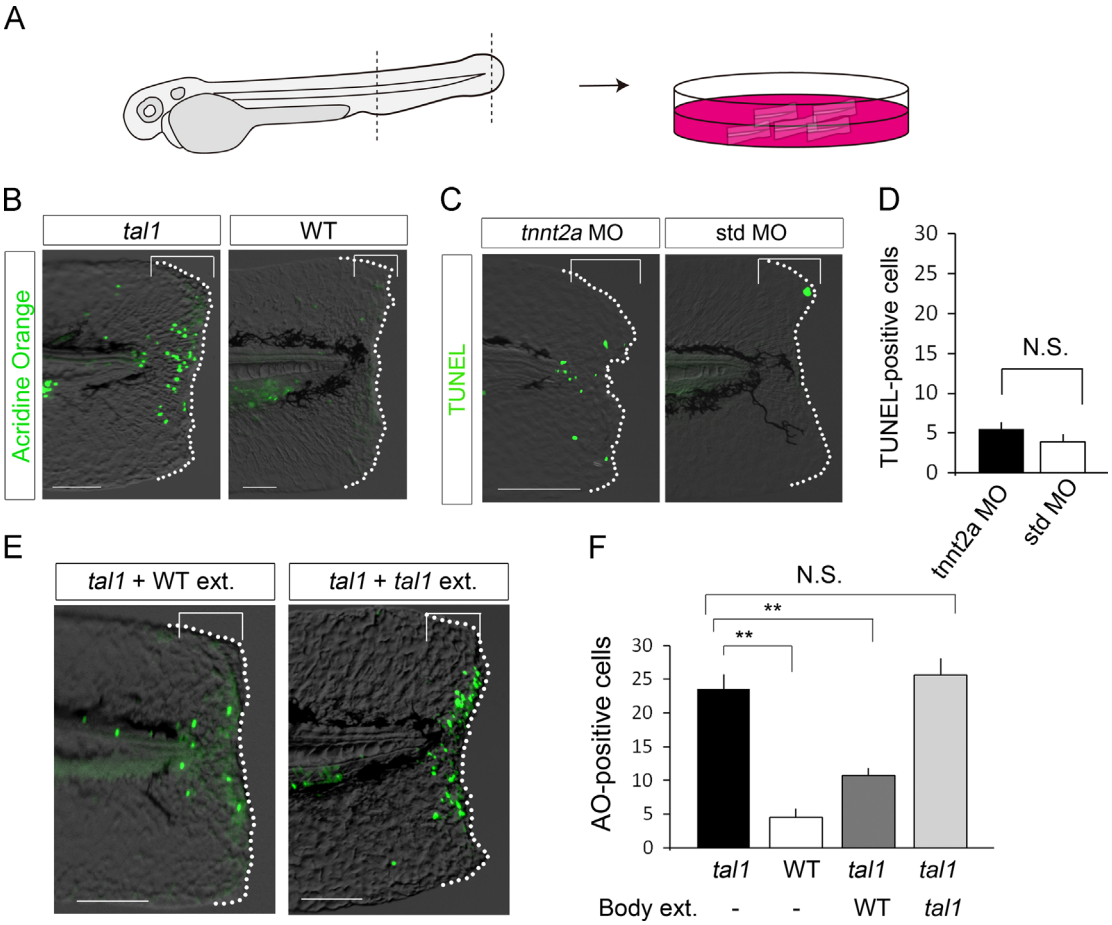

Fig. 6. Rescue of apoptosis with the wild-type body extract. (A) Procedure of tail explant culture. Following fin fold amputation, the tail tissue was isolated and placed in the culture medium. At 12 hpa, acridine orange staining was performed to detect apoptotic cells. (B) Reproduction of the blastema apoptosis phenotype in the tail explant. Blastema apoptosis was detected in the mutant explant, but not in the wild-type one. (C) Detection of TUNEL-positive cells in the *tnnt2a*/*silent heart* morphant. Although almost all morphants did not have the heartbeat, no significant induction of apoptosis was observed. $n=50$ (*tnnt2a* MO) and 17 (standard control MO), respectively. (D) Quantification of the number of TUNEL-positive cells (brackets) in (C). (E) Rescue of the apoptosis in the *tal*1 mutant with the wild-type extract, but not the mutant one. Similar results were obtained more than three independent experiments. (F) Quantification of the number of TUNEL-positive cells in the explant culture. $n=15$ (*tal*1), 14 (WT), 13 (*tal*1 + WT body fluid), and 14 (*tal*1 + *tal*1 body fluid), respectively. Data in (D) and (F) are presented as mean ± s.e.m. Statistical significance was tested using Welch's *t* test. $^{**}P<0.001$. N.S., not significant. The dotted lines in (B), (C) and (E) indicate the outline of the fin fold. Scale bars represent 100 μm.

In this study, we showed that the myeloid cells are indispensable for the survival of primed regenerative cells. This does not rule out the involvement of other hematopoietic cells and endothelial cells for the survival of regenerative cells, but in accordance with our result, a number of reports have suggested the important relationship between myeloid lineage cells and regeneration. A recent study by Petrie et al. (2014) showed that ablation of macrophages during adult fin regeneration reduces blastema cell proliferation and causes abnormal regeneration. Although these studies did not inspect apoptosis during regeneration, the decrease of survival factor could be a cause of the regeneration defects observed in these studies.

Other recent studies have suggested the role of myeloid cells for attenuating the ROS signaling during regeneration. Upon tissue traumas, the hydrogen peroxide (H_2O_2) is generated from the injured cells, and neutrophils sense it to migrate to the wound site (Niethammer et al., 2009). Intriguingly, Pase et al. (2012) has shown using the fin fold model that the neutrophil-derived Myeloperoxidase (Mpx) down-regulate the H_2O_2 burst following wounding. Since it has been suggested that the ROS signaling during early regeneration stage relates to apoptosis and JNK activation in the epidermis during adult fin regeneration (Gauron et al., 2013), an excess and prolonged ROS signaling caused by the loss of myeloid cells in the *clo*/*tal*1 mutants could be a cause of apoptosis of regenerative cells, and the Mpx could be a candidate of the survival factor. However, this is unlikely, because inhibitors against ROS or JNK signals did not affect the apoptosis phenotype in the mutants (Supplementary Fig. S4). Furthermore, the Mpx is a large protein of 150 kD consisting of two light and two heavy chains, which is thought to be sensitive to heat treatment, but as

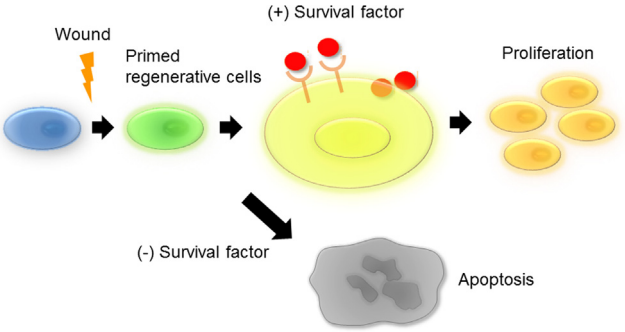

Fig. 7. A schematic diagram of the mechanism for the survival of primed regenerative cells. The cells activated by a wound signal (primed regenerative cells) are susceptible to apoptosis, but the survival factor derived from the myeloid cells prevented the apoptosis and support the survival and cell proliferation.

we demonstrated, the survival factor appears to be a heat-stable substance (Supplementary Fig. S10).

After all, the entity of survival factor for regenerative cells is still an open question. So far, only a few examples of such long-range regulators that influence the tissue homeostasis have been known. In an intriguing example, recent studies have shown that Growth differentiation factor 11 (Gdf11), a myostatin-homologous protein, mediates the rejuvenation of neuronal and muscle stem cells (Katsimpardi et al., 2014; Sinha et al., 2014). Such factors including the survival factor revealed in this study may tune the regenerative abilities depending on age, tissue, and nutritional statuses.

Conclusions

Our research has shown that the survival of primed regenerative tissue is normally supported by a factor derived from the hematopoietic tissues, mainly the myeloid cells. Unlike many of signals and molecules that are induced on site and required for regeneration, our study firstly revealed the existence of factor that acts from a distance to regulate tissue regeneration. The study of the molecular identity of such a factor would be a fascinating subject of future research.

Acknowledgments

We thank D. Stainier (Max Planck Institute) for kindly providing the *clo*^{la1164}, L.I. Zon for *tal*1, M. Kobayashi (Tsukuba University) for the *vlad tepes*, A. Sehara (Kyoto University) for Tg(*fli*1:EGFP), and T.A. Look (Harvard University) for the *pCS2-EGFP-bcl2* construct. *tp*53 mutant zebrafish was obtained from the ZIRC.

Appendix A. Supporting information

Supplementary data associated with this article can be found in the online version at http://dx.doi.org/10.1016/j.ydbio.2014.12.015.

References

Berghmans, S., Murphey, R.D., Wienholds, E., Neuberg, D., Kutok, J.L., Fletcher, C.D., Morris, J.P., Liu, T.X., Schulte-Merker, S., Kanki, J.P., Plasterk, R., Zon, L.I., Look, A.T., 2005. tp53 mutant zebrafish develop malignant peripheral nerve sheath tumors. Proc. Natl. Acad. Sci. USA 102, 407–412.

Blum, N., Begemann, G., 2012. Retinoic acid signaling controls the formation, proliferation and survival of the blastema during adult zebrafish fin regeneration. Development 139, 107–116.

Bussmann, J., Bakkers, J., Schulte-Merker, S., 2007. Early endocardial morphogenesis requires Scl/Tal1. PLoS Genet. 3, e140.

Campbell, L.J.,, Crews, C.M., 2008. Wound epidermis formation and function in urodele amphibian limb regeneration. Cell. Mol. Life Sci. 65, 73–79.

Chablais, F., Jazwinska, A., 2010. IGF signaling between blastema and wound epidermis is required for fin regeneration. Development 137, 871–879.

Chan, J., Bayliss, P.E., Wood, J.M., Roberts, T.M., 2002. Dissection of angiogenic signaling in zebrafish using a chemical genetic approach. Cancer Cell 1, 257–267.

Gauron, C., Rampon, C., Bouzaffour, M., Ipendey, E., Teillon, J., Volovitch, M., Vriz, S., 2013. Sustained production of ROS triggers compensatory proliferation and is required for regeneration to proceed. Scientific Rep 3, 2084.

Grotek, B., Wehner, D., Weidinger, G., 2013. Notch signaling coordinates cellular proliferation with differentiation during zebrafish fin regeneration. Development 140, 1412–1423.

Ishida, T., Nakajima, T., Kudo, A., Kawakami, A., 2010. Phosphorylation of Junb family proteins by the Jun N-terminal kinase supports tissue regeneration in zebrafish. Developmental Biol. 340, 468–479.

Jaźwińska, A., Badakov, R., Keating, M.T., 2007. Activin-βA signaling is required for zebrafish fin regeneration. Curr. Biol. 17, 1390–1395.

Jing, L., Zon, L.I., 2011. Zebrafish as a model for normal and malignant hematopoiesis. Dis. Model. Mech 4, 433–438.

Katsimpardi, L., Litterman, N.K., Schein, P.A., Miller, C.M., Loffredo, F.S., Wojtkiewicz, G.R., Chen, J.W., Lee, R.T., Wagers, A.J., Rubin, L.L., 2014. Vascular and neurogenic rejuvenation of the aging mouse brain by young systemic factors. Science 344, 630–634.

Kawakami, A., Fukazawa, T., Takeda, H., 2004. Early fin primordia of zebrafish larvae regenerate by a similar growth control mechanism with adult regeneration. Developmental Dyn. 231, 693–699.

Kroemer, G., Galluzzi, L., Vandenabeele, P., Abrams, J., Alnemri, E.S., Baehrecke, E.H., Blagosklonny, M.V., El-Deiry, W.S., Golstein, P., Green, D.R., Hengartner, M., Knight, R.A., Kumar, S., Lipton, S.A., Malorni, W., Nuñez, G., Peter, M.E., Tschopp, J., Yuan, J., Piacentini, M., Zhivotovsky, B., Melino, G., 2008. Classification of cell death: recommendations of the nomenclature committee on cell death 2009. Cell Death Differentiation 16, 3–11.

Langenau, D.M., Jette, C., Berghmans, S., Palomero, T., Kanki, J.P., Kutok, J.L., Look, A.T., 2005. Suppression of apoptosis by bcl-2 overexpression in lymphoid cells of transgenic zebrafish. Blood 105, 3278–3285.

Liao, W., Ho, C.Y., Yan, Y.L., Postlethwait, J., Stainier, D.Y., 2000. Hhex and scl function in parallel to regulate early endothelial and blood differentiation in zebrafish. Development 127, 4303–4313.

Love, N.R., Chen, Y., Ishibashi, S., Kritsiligkou, P., Lea, R., Koh, Y., Gallop, J.L., Dorey, K., Amaya, E., 2013. Amputation-induced reactive oxygen species are required for successful Xenopus tadpole tail regeneration. Nat. Cell. Biol. 15, 222–228.

Lyons, S.E., Lawson, N.D., Lei, L., Bennett, P.E., Weinstein, B.M., Liu, P.P., 2002. A nonsense mutation in zebrafish gata1 causes the bloodless phenotype in vlad tepes. Proc. Natl. Acad. Sci. USA 99, 5454–5459.

Mathew, L.K., Sengupta, S., Kawakami, A., Andreasen, E.A., Lohr, C.V., Loynes, C.A., Renshaw, S.A., Peterson, R.T., Tanguay, R.L., 2007. Unraveling tissue regeneration pathways using chemical genetics. J. Biol. Chem. 282, 35202–35210.

Miura, M., 2011. Active participation of cell death in development and organismal homeostasis. Development Growth Differentiation 53, 125–136.

Mohamad, N., Gutiérrez, A., Nunez, M., Cocca, C., Martin, G., Cricco, G., Medina, V., Rivera, E., Bergoc, R., 2005. Mitochondrial apoptotic pathways. Biocell 29, 149–161.

Munch, J., Gonzalez-Rajal, A., de la Pompa, J.L., 2013. Notch regulates blastema proliferation and prevents differentiation during adult zebrafish fin regeneration. Development 140, 1402–1411.

Niethammer, P., Grabher, C., Look, A.T., Mitchison, T.J., 2009. A tissue-scale gradient of hydrogen peroxide mediates rapid wound detection in zebrafish. Nature 459, 996–999.

Padhi, B.K., Joly, L., Tellis, P., Smith, A., Nanjappa, P., Chevrette, M., Ekker, M., Akimenko, M.A., 2004. Screen for genes differentially expressed during regeneration of the zebrafish caudal fin. Developmental Dyn. 231, 527–541.

Pase, L., Layton, J.E., Wittmann, C., Ellett, F., Nowell, C.J., Reyes-Aldasoro, C.C., Varma, S., Rogers, K.L., Hall, C.J., Keightley, M.C., Crosier, P.S., Grabher, C., Heath, J.K., Renshaw, S.A., Lieschke, G.J., 2012. Neutrophil-delivered myeloperoxidase dampens the hydrogen peroxide burst after tissue wounding in zebrafish. Curr. Biol. 22, 1818–1824.

Petrie, T.A., Strand, N.S., Tsung-Yang, C., Rabinowitz, J.S., Moon, R.T., 2014. Macrophages modulate adult zebrafish tail fin regeneration. Development 141, 2581–2591.

Poss, K.D., Shen, J., Nechiporuk, A., McMahon, G., Thisse, B., Thisse, C., Keating, M.T., 2000. Roles for Fgf signaling during zebrafish fin regeneration. Developmental Biol. 222, 347–358.

Quint, E., Smith, A., Avaron, F., Laforest, L., Miles, J., Gaffield, W., Akimenko, M.A., 2002. Bone patterning is altered in the regenerating zebrafish caudal fin after ectopic expression of sonic hedgehog and bmp2b or exposure to cyclopamine. Proc. Natl. Acad. Sci. USA 99, 8713–8718.

Rhodes, J., Hagen, A., Hsu, K., Deng, M., Liu, T.X., Look, A.T., Kanki, J.P., 2005. Interplay of pu.1 and gata1 determines myelo-erythroid progenitor cell fate in zebrafish. Developmental Cell 8, 97–108.

Sakaguchi, T.F., Sadler, K.C., Crosnier, C., Stainier, D.Y., 2008. Endothelial signals modulate hepatocyte apicobasal polarization in zebrafish. Curr. Biol. 18, 1565–1571.

Schebesta, M., Lien, C.L., Engel, F.B., Keating, M.T., 2006. Transcriptional profiling of caudal fin regeneration in zebrafish. Scientific World Journal 6 (Suppl 1), 38–54.

Sehnert, A.J., Huq, A., Weinstein, B.M., Walker, C., Fishman, M., Stainier, D.Y., 2002. Cardiac troponin T is essential in sarcomere assembly and cardiac contractility. Nat. Genet. 31, 106–110.

Sinha, M., Jang, Y.C., Oh, J., Khong, D., Wu, E.Y., Manohar, R., Miller, C., Regalado, S.G., Loffredo, F.S., Pancoast, J.R., Hirshman, M.F., Lebowitz, J., Shadrach, J.L., Cerletti, M., Kim, M.J., Serwold, T., Goodyear, L.J., Rosner, B., Lee, R.T., Wagers, A.J., 2014. Restoring systemic GDF11 levels reverses age-related dysfunction in mouse skeletal muscle. Science 344, 649–652.

Smith, A., Avaron, F., Guay, D., Padhi, B.K., Akimenko, M.A., 2006. Inhibition of BMP signaling during zebrafish fin regeneration disrupts fin growth and scleroblast differentiation and function. Developmental Biol. 299, 438–454.

Stainier, D.Y., Weinstein, B.M., Detrich 3rd, H.W., Zon, L.I., Fishman, M.C., 1995. Cloche, an early acting zebrafish gene, is required by both the endothelial and hematopoietic lineages. Development 121, 3141–3150.

Stoick-Cooper, C.L., Weidinger, G., Riehle, K.J., Hubbert, C., Major, M.B., Fausto, N., Moon, R.T., 2007. Distinct Wnt signaling pathways have opposing roles in appendage regeneration. Development 134, 479–489.

Thisse, C., Thisse, B., 2008. High-resolution in situ hybridization to whole-mount zebrafish embryos. Nat. Protoc. 3, 59–69.

Vousden, K.H., 2000. p53: death star. Cell 103, 691–694.

Vousden, K.H., Lane, D.P., 2007. p53 in health and disease. Nat. Rev. Mol. Cell Biol. 8, 275–283.

Yoo, S.K., Freisinger, C.M., LeBert, D.C., Huttenlocher, A., 2012. Early redox, Src family kinase, and calcium signaling integrate wound responses and tissue regeneration in zebrafish. J. Cell Biol. 199, 225–234.
Yoshinari, N., Ando, K., Kudo, A., Kinoshita, M., Kawakami, A., 2012. Colored medaka and zebrafish: transgenics with ubiquitous and strong transgene expression driven by the medaka β-actin promoter. Development Growth Differentiation 54, 818–828.
Yoshinari, N., Ishida, T., Kudo, A., Kawakami, A., 2009. Gene expression and functional analysis of zebrafish larval fin fold regeneration. Developmental Biol. 325, 71–81.